By: Sanjit Bhowmick, Ph.D., Hysitron, Inc. and Matthew M. Nowell, EDAX, Inc.

Mechanical Properties of Ferrite and Austenite Phases in Duplex Steel: A Combined EBSD and SEM Nanoindentation Study

Duplex Stainless Steel 2205

Duplex 2205 is a two-phase, ferritic (α) and austenitic (γ) stainless steel alloyed with 22% Cr, 3% Mo, and 5 to 6% Ni. It is characterized by good fatigue strength, outstanding resistance to stress corrosion cracking, and general corrosion in severe environments. Duplex steel offers very high yield strength compared to the standard austenitic stainless steel. The main application for duplex steel is chemical processing, transport, storage, pressure vessels, tanks, oil field piping, and heat exchangers. The present work aims to distinguish ferrite and austenite phases present in duplex steel using Electron Backscatter Diffraction (EBSD) and determine mechanical properties of individual phases via in-situ nanoindentation with the PI 87 Scanning Electron Microscope (SEM) PicoIndenter.

PI 87 SEM PicoIndentor®

The PI 87 SEM PicoIndenter is a depth-sensing nanomechanical test instrument that is specifically designed to leverage the advanced imaging capabilities of modern scanning electron microscopes (SEM, FIB/SEM). Flexible sample positioning with five degrees of freedom (X, Y, Z, tilt, rotation) provides the user the ability to align the sample with an ion beam for sample preparation or detectors such as EBSD, Energy Dispersive Spectroscopy (EDS), or Wavelength Dispersive Spectrometry (WDS) to obtain a deeper understanding of a material's mechanical response.

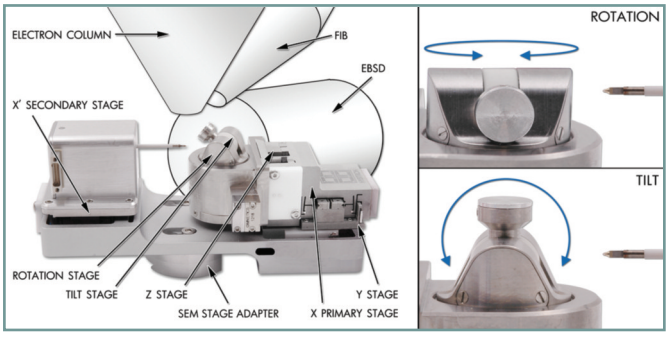

Figure 1. A schematic of the PI 87 SEM PicoIndenter in an SEM (left), and its advanced rotatation (top right) and tilt (bottom right) stages.

Electron Backscatter Diffraction (EBSD)

EBSD has developed into a well-established microstructural characterization technique that provides quantifiable information on the grain size and shape, grain boundary character, preferred orientation, and local strain state of crystalline materials. Recent developments in pattern detection technology have increased EBSD data acquisition rates to more than 1,400 patterns/second, reducing the time required to obtain quality EBSD images, making this technique the perfect complement to high resolution mechanical testing, such as nanoindentation.

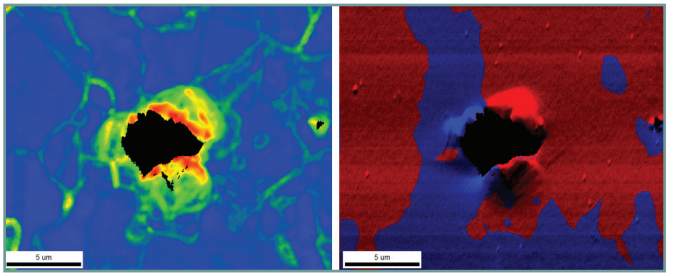

Figure 2. EBSD phase map (right), ferrite in blue and autenite in red, and local orientation spread map (left) show the amount of plastic strain field developed by an indent varies between phases.

Experimental Procedure

A polished sample of duplex steel was attached to a microscopy stub with conductive adhesive, and mechanically secured in the staging of the PI 87. Using the enhanced tilt and rotation capabilities of the PI 87, the sample was aligned with the EDAX EBSD camera for grain and phase mapping using TEAM™ software. After mapping, the sample was re-oriented with the indentation probe, and load-controlled nanoindentation tests were conducted to peak loads of 1, 2, and 5 mN. At the conclusion of the mechanical tests, the sample was again aligned with the EBSD detector to map the regions where the indentations were performed.

EBSD-Enhanced Nanoindentation Results

Figure 3 shows a Pattern Region of Interest Analysis System (PRIAS) image, inverse pole figure (IPF) map, and a phase map that were obtained after conducting nanoindentation experiments on individual phases and interfaces. EBSD maps show that the sample has similar volume fractions of both the ferritic and austenitic phases.

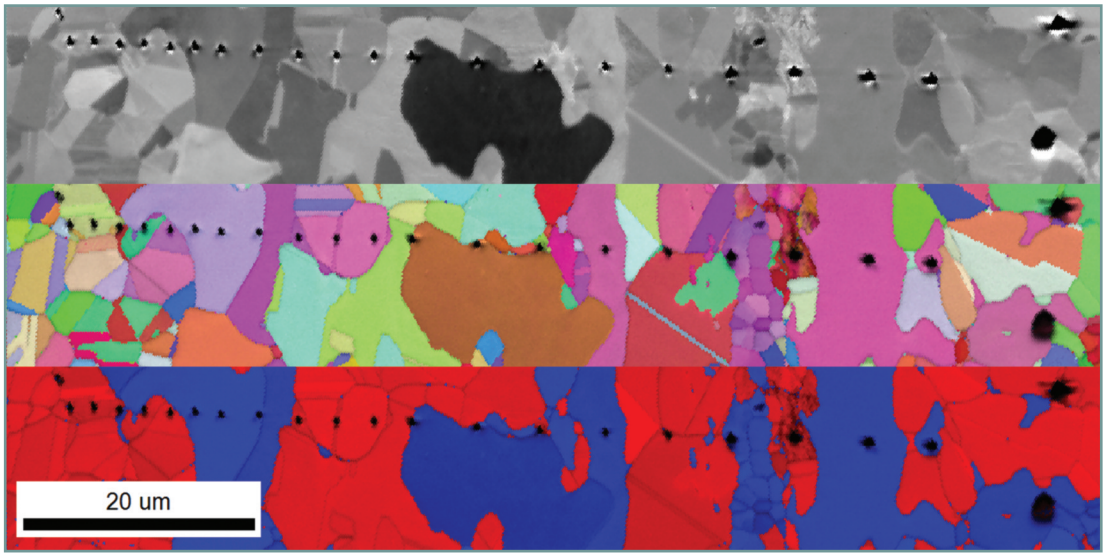

Figure 3. PRIAS image of indentations and microstructure (top), IPF map (middle), and phase map (bottom).

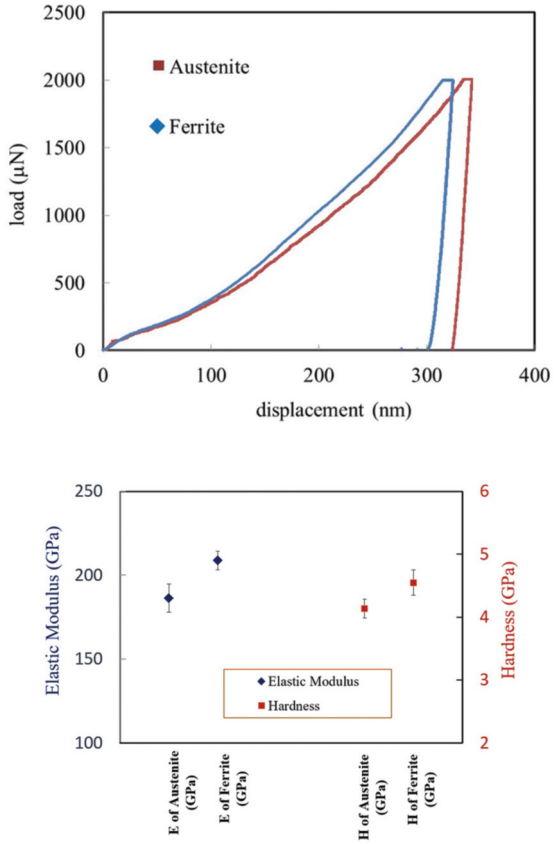

Figure 4. Typical P-h curves from austentic and ferritic phases (top), elastic modulus and hardness variation in ferrite and austenite (bottom).

The local elastic and plastic properties of the phase domains were determined from load-displacement curves by analyzing 5 to 8 indentations from each phase. The elastic moduli (E) were measured to be 208.7 +/- 5.5 GPa and 186.3 +/- 8.3 GPa for the ferritic and austenitic phases, respectively. The hardness values (H) show a similar trend with values of 4.6 +/- 0.20 GPa for ferrite and 4.1 +/- 0.15 GPa for austenite. Although the actual numbers vary slightly with the results reports by Gadelrab et al., Campos et al., and Guo et al., the relative difference in the mechanical properties of the two phases agrees well with the trends reported in the previous studies. Also, the results confirm the expected enhancement provided by solid solution hardening of Ni and Mo in the ferrite phase.

References

1. K. Gadelrab, G. Li, M. Chiesa, and T. Souier, J. Mater. Res., 27 (2012), 1573.
2. M. Campos, A. Bautista, D.Caceres, J. Abenojar, J.M. Torralba, J. of the European Ceramic Society 23 (2003) 2813.
3. L. Q. Guo, M. C. Lin, L. J. Qiao, A. A. Volinsky, Applied Surface Sci., 287 (2013) 499.

Conclusion

Using the PI 87 in conjunction with EBSD enables a more robust characterization of metallic materials by combining high resolution phase and grain orientation mapping capabilities with targeted nanomechanical property measurements. This combination could also be used to extend the scope of research related to other advanced textured, anisotropic, or multi-phase materials.

© EDAX Inc., 2016 May